Computer Aided Design of Square Spiral Transformers and Inductors

by

E. Frlan*, S. Meszaros, M. Cuhaci and J.S. Wight*

Communications Research Centre
Ottawa, Ontario

*Carleton University
Ottawa, Ontario

ABSTRACT

A simple, yet accurate, lumped element model for four-port planar rectangular spiral structures has been developed. Closed form expressions were used to generate frequency dependent parameter values, resulting in an equivalent circuit which is easily incorporated into existing analysis packages. The technique has been applied to standard and centre-tapped transformer configurations, and has also been modified to accurately analyze spiral inductors to 20 GHz. Comparison with measured results has shown good agreement up to the first resonant frequency of the structures.

INTRODUCTION

The planar spiral transformer has a wide variety of potential applications as a coupling and/or impedance transforming component in MMIC (Monolithic Microwave Integrated Circuit) and MHMIC (Miniature Hybrid Microwave Integrated Circuit) designs. Its use as a matching element in a balanced amplifier topology has been reported by Jamison et al. [1], while Ferguson et al. [2] have extended its use to an image rejection mixer, taking advantage of a "wraparound" layout technique to conserve real-estate. However, very little has been published to date on the analysis of such transformers. Wiemer et al. [3] have described a technique based on multiconductor line theory, in which each side of the transformer is subdivided into a cascade of multiports and then evaluated by an enhanced spectral domain technique.

The present work is based on a lumped element approach and does not require look-up tables. The result is a simpler model which is easily integrated into existing software packages such as SuperCompact™ for use in overall circuit analysis and optimization.

ANALYSIS

The objective of the analysis is to calculate values for the lumped element equivalent circuit shown in Figure 1, based on the physical parameters of the transformer. Since the structure will be a significant fraction of a wavelength at high frequencies and the conductor thickness is comparable to the skin depth, the model must incorporate frequency dependent elements.

The rectangular spiral transformer is partitioned into line segments as shown for a sample case in Figure 2. The static self-inductance and mutual inductance between all parallel line segments are calculated following the method described by Greenhouse [4] where it is assumed that perpendicular segments have negligible mutual inductance. The direction of current through the transformer dictates the sign of the mutual inductance between segments. For example, in Figure 2 it can be seen that $M_{1,10}$ is positive and $M_{1,3}$ is negative.

Greenhouse uses the geometric mean distance (GMD) of the conductor cross-section to incorporate the non-zero metallization thickness in the self-inductance calculation. The GMD for a conductor of rectangular cross-section is given by equation 1.

$$GMD = 0.2235 \times (Width + Thickness) \qquad (1)$$

The finite thickness effect may be neglected in the mutual inductance terms. Note that the frequency dependent internal inductance term arising from changing current densities is assumed to be negligible in this analysis. However, as shown by Krafesik and Dawson [5], the differential phase shift introduced between the various segments as frequency increases must be included, as it affects both the mutual and, to a lesser extent, the self inductance terms. In addition, the mutual inductance caused by a fictional mirror image structure must be included for those transformers fabricated with a ground plane. The significantly lower net inductance in this case is accounted for by the reverse current flow in the image.

CH2725-0/89/0000-0661$01.00 © 1989 IEEE

The total primary inductance for the example shown is given by:

$$L_1 = \sum_{i=1}^{6} L_i + \sum_{i=1}^{6}\sum_{j=1}^{6} M_{ij}, \qquad (2)$$

the total secondary inductance is given by:

$$L_2 = \sum_{i=7}^{12} L_i + \sum_{i=7}^{12}\sum_{j=7}^{12} M_{ij} \qquad (3)$$

and the mutual inductance between primary and secondary is given by:

$$M = \frac{\sum_{i=1}^{6}\sum_{7}^{12} M_{ij}}{2}. \qquad (4)$$

In equation 4, the sum of all the mutual inductances between the primary and secondary of the transformer is divided by two in order to avoid counting the mutual inductance between two line segments in the lumped circuit transformers twice.

Calculation of the segment-to-ground capacitance and the mutual interline capacitance is based on the even- and odd-mode analysis of Smith [6]. The capacitance between non-adjacent lines can be neglected with little change in the final accuracy of the model, unlike the total inductance in which all the individual self inductances must be considered. The variation in phase shift with frequency also produces a change in the effective mutual capacitance, C_m, between the primary and secondary. The value of C_m at DC is effectively zero, but as the frequency increases its effect on the parameters calculated by the model becomes significant.

Determination of the equivalent resistances of the primary and secondary spirals, R1 and R2 respectively, is complicated by the fact that the skin depth is no longer negligible compared to the conductor thickness for typical thin-film technologies. Detailed numerical techniques have been developed for exact resistance results by Waldo and Wolff [7]. This study has found that the closed form expression given by Pettenpaul et al. [8] describes the frequency dependent resistance sufficiently. The effect of dielectric losses for the substrates used in this study is negligible compared to conductor losses.

The discontinuity effect of the corner chamfers on the structures is not very significant at low frequencies. However, in order to include this effect at higher frequencies, closed form equations as described by Kirschning et al. [9] are used in the models. The coupling between chamfers is not taken into account.

The response of centre-tapped transformers and inductors can be derived using a similar procedure and so they are not described separately in this article.

FABRICATION

Transformers and inductors were fabricated on 0.010" alumina and 0.020" quartz substrates using thin-film techniques. The first level metal was composed of 1 μm gold evaporated onto a Ti:W seed layer, while the airbridges were selectively plated up to a thickness of 4 μm. A typical layout of one of the centre-tapped transformers is shown in Figure 3, together with a schematic. Coplanar probing pads allowed RF testing of ports 1 and 2, while ports 3 and 4 were grounded, and port 5 was terminated in a 50 Ω load. Other transformers were laid out as shown in Figure 4, with both primary and secondary grounded.

MEASURED AND CALCULATED RESULTS

The results for a 455 μm x 455 μm centre-tapped transformer, with 20 μm width and 10 μm spacing, on 0.020" quartz (Figure 3) are shown in Figure 5. The lower input return loss seen below 10 GHz is partially caused by mismatch due to the impedance transformation. The model is very accurate below the first resonant frequency at 18 GHz. Above resonance, the dominant coupling mechanism becomes capacitive and the structure shows a maximum power transfer with 1.9 dB insertion loss.

Good agreement up to 20 GHz, between the predicted and measured results, was also found for square spiral transformers. As an example, a 265 μm x 245 μm square spiral transformer, with 10 μm width and spacing, on 0.010" alumina are shown in Figure 6. Due to the smaller overall dimensions of this transformer as compared to the previous one, inductive coupling is observed over the entire frequency range. Maximum power transfer to the output port occurs at approximately 7 GHz.

A program which calculates the Y-parameters of the equivalent four-port has been written. The effects of changing track width, spacing, and the overall lengths of the primary and secondary can easily be observed allowing the tradeoff between the amount of inductive coupling and the structure losses to be evaluated. It was observed that the frequency at which peak inductive coupling to the output occurs is also sensitive to track width and spacing.

Overall, the most sensitive components of the transformer model were found to be M and C_m. If these equivalent circuit components are not calculated accurately, the resonant frequency response of the model is severely affected. The model is found to be fairly insensitive to the self inductances of the primary and secondary as well as the capacitance to ground. Also, the final calculated response of the transformer demonstrates little

sensitivity to resistive losses.

For the centre-tapped transformer, our investigation shows that the model is less accurate at and above resonance. This is believed to be caused by the coupling to the coplanar ground strip which is not taken into account in the analysis. Future work will include the development of via holes to avoid the need for ground connections between the input and output ports. In addition, a small error was introduced by considering the airbridge as a simple transmission line and ignoring the capacitive coupling effect of the overpass to the tracks.

The above analysis has also been adapted to square spiral inductors. Measured and calculated results for a 2-1/2 turn inductor, fabricated on 0.010" alumina with an inner diameter of 160 μm and line and space widths of 20 μm and 10 μm respectively, are shown in Figure 7. This structure has a calculated inductance of 2.0 nH at low frequencies and this decreases to 1.75 nH at 20 GHz, illustrating the effect of phase shift on this parameter. The inductor model predicts device behaviour quite well up to and beyond resonance.

CONCLUSION

A simple frequency dependent lumped element model has been described which predicts the characteristics of planar spiral transformers and inductors accurately to 20 GHz. The method outlined can easily be implemented in a commercial microwave CAD program allowing its use in the optimization of various types of active circuits. The spiral inductor model has been incorporated into SuperCompact™ as a user-defined model. Work is ongoing to incorporate the transformer models and to extend the analysis to higher frequencies.

REFERENCES

[1] S.A.Jamison, A.Podell, M.Helix, P.Ng, C.Chao "Inductively Coupled Push-Pull Amplifiers for Low Cost Monolithic Microwave ICs", 1982 IEEE GaAs IC Symposium, pp. 91-93.

[2] D.Ferguson, P.Bauhahn, J.Keuper, R.Lokken, J.Culp, C.Chao, A.Podell " Transformer Coupled High-Density Circuit Technique for MMIC", 1984 IEEE MTT-S Digest, pp. 34-36.

[3] L.Wiemer, R.H.Jansen, I.D.Robertson, J.B.Swift "Computer Simulation and Experimental Investigation of Square Spiral Transformers for MMIC Applications", IEE Colloquium on "Computer Aided Design of Microwave Circuits", Digest No. 99, Nov. 11, 1985, p. 2/1-5.

[4] H. M. Greenhouse, "Design of Planar Rectangular Microelectronic Inductors", IEEE Transaction on Parts, Hybrids and Packaging, PHP-10, No. 2, June 1974, pp. 101-109.

[5] D. Krafesik and D. Dawson, "A Closed-Form Expression for Representing the Distributed Nature of the Spiral Inductor", 1986 IEEE MTT Monolithic Circuits Symposium Digest, pp. 87-91.

[6] J. I. Smith, "The Even- and Odd-Mode Capacitance parameters for Coupled Lines in Suspended Substrate", IEEE Microwave Theory and Tech., MTT-19, No. 5, May 1971, pp. 424-431.

[7] P. Waldo and I. Wolff, "Dual Bounds Variational Formulation of Skin Effect Problem", 1986 IEEE MTT-S Digest, pp.333-336.

[8] E.Pettenpaul, H.Kapusta, A.Weisgerber, H.Mampe, J.Luginsland, I.Wolff "CAD Models of Lumped Elements on GaAs Up to 18 GHz", IEEE Trans. on Microwave Theory and Techniques, MTT-36, No. 2, February 1988, pp. 294-304.

[9] M.Kirschning, R.H.Jansen, N.H.L.Koster "Measurement and Computer-Aided Modeling of Microstrip Discontinuities by an Improved Resonator Method", 1983 IEEE MTT-S Digest, pp.495-497.

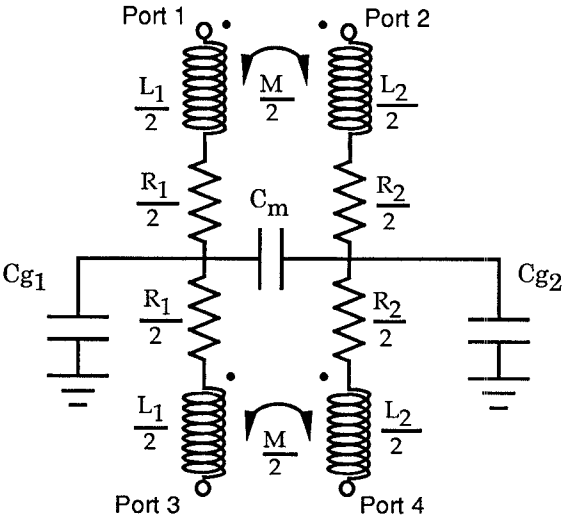

Figure 1: Transformer Lumped Element Equivalent Model

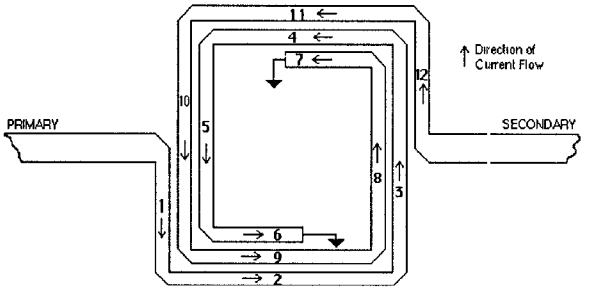

Figure 2: Sample Transformer Partitioned into Segments

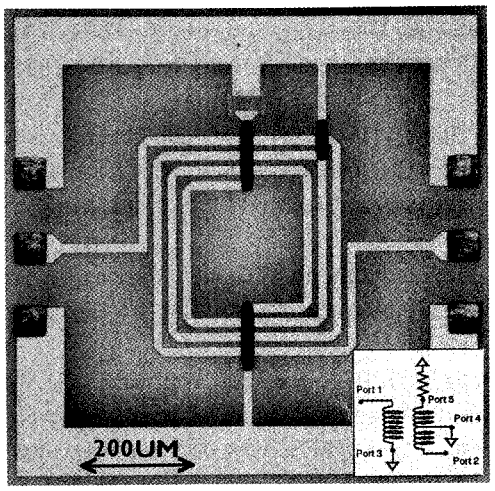

Figure 3: Photograph of 1-3/4 Center-Tapped Transformer

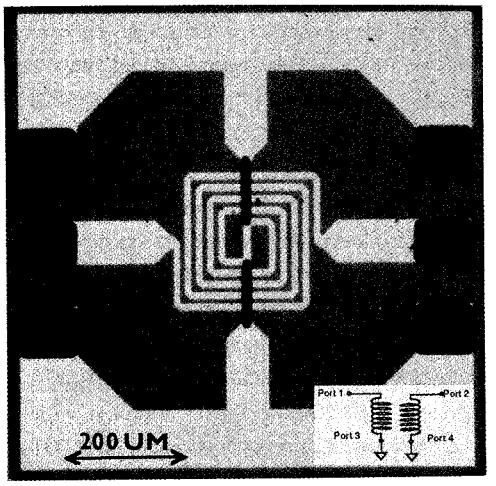

Figure 4: Photograph of 2-1/2 Turn Square Transformer

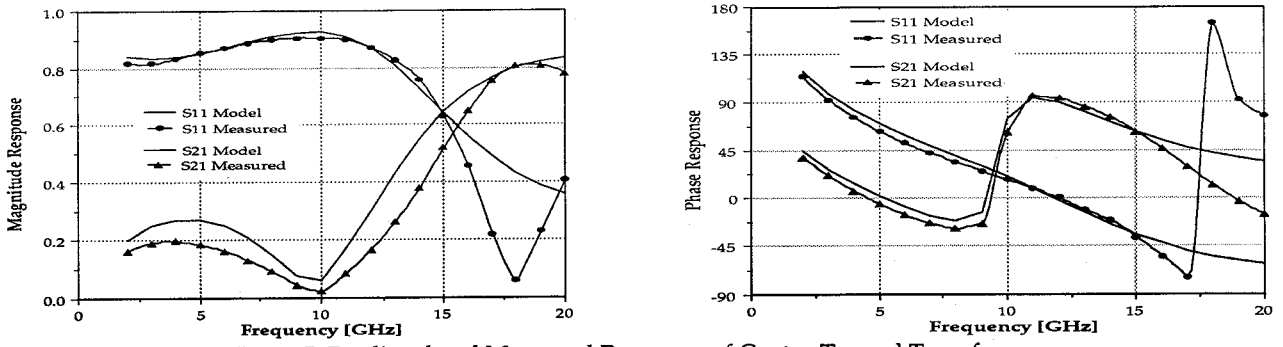

Figure 5: Predicted and Measured Response of Center-Tapped Transformer

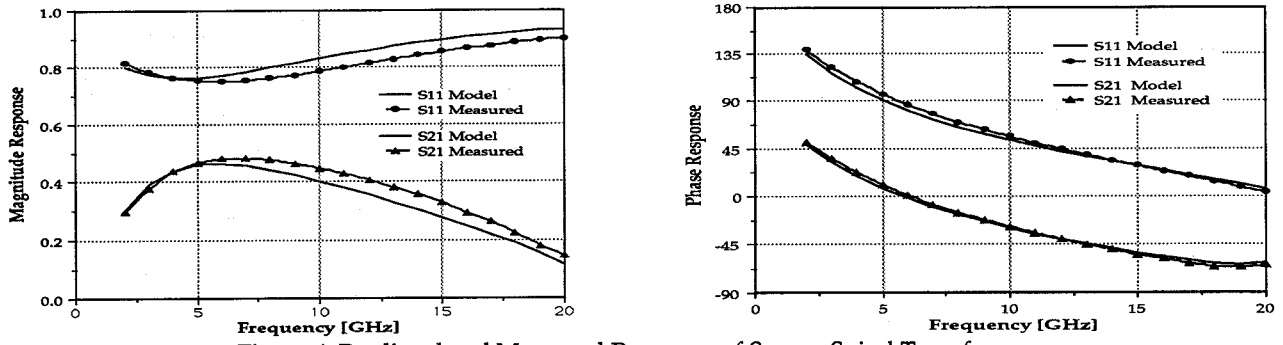

Figure 6: Predicted and Measured Response of Square Spiral Transformer

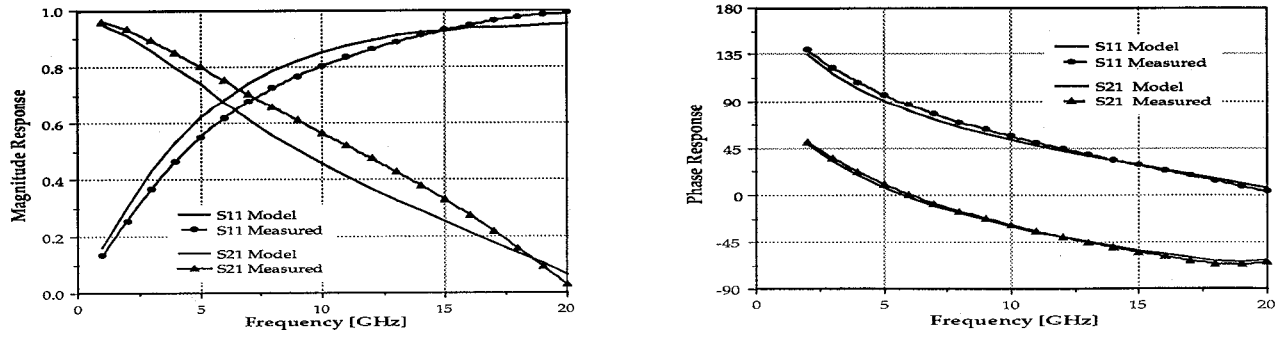

Figure 7: Predicted and Measured Response of Square Spiral Inductor